Med Chem Res (2016) 25:539–552
DOI 10.1007/s00044-016-1504-3

MEDICINAL CHEMISTRY RESEARCH

ORIGINAL RESEARCH

Design and development of oxobenzimidazoles as novel androgen receptor antagonists

R. Elancheran[1] · K. Saravanan[2] · Bhaswati Choudhury[1] · S. Divakar[3] · S. Kabilan[2] · M. Ramanathan[3] · Babulal Das[4] · R. Devi[1] · Jibon Kotoky[1]

Received: 5 February 2015 / Accepted: 6 January 2016 / Published online: 21 January 2016

Abstract Antiandrogens are a novel class of anticancer agents that inhibit cancer cell proliferation and induce apoptosis in various cell lines. To find the lead compound from the oxobenzimidazole derivatives, receptor-ligand docking studies were initially performed using Schrödinger software. The best fit molecules were synthesized and characterized through IR, ^{1}H-NMR, ^{13}C-NMR and HRMS analyses. The structure of compound **(9b)** was further confirmed by single-crystal XRD analysis. The cell viability of the compounds was determined by MTT assay to find IC_{50} values against prostate cancer and breast cancer cell lines (PC-3, LNCaP, MCF-7 and MDA-MB-231). The ADME/T property studies were performed to rationalize the inhibitory properties of these compounds. It can be concluded from the study that **9b** is the most active compound from the series against PC-3 and LNCaP cell lines.

Keywords Androgen receptor · Prostate cancer · Antiandrogen · Breast cancer · Oxobenzimidazoles

Electronic supplementary material The online version of this article (doi:10.1007/s00044-016-1504-3) contains supplementary material, which is available to authorized users.

✉ Jibon Kotoky
jkotoky@gmail.com

[1] Drug Discovery Laboratory, Life Sciences Division, Institute of Advanced Study in Science and Technology, Guwahati, Assam 781035, India

[2] Department of Chemistry, Annamalai University, Annamalai Nagar, Tamilnadu 608002, India

[3] Department of Pharmacology, PSG College of Pharmacy, Coimbatore, Tamilnadu 641 004, India

[4] Department of Chemistry, Indian Institute of Technology, Guwahati, Assam 781035, India

Introduction

Androgen receptor (AR), belongs to the nuclear receptor subfamily, plays an important role in the development, growth, function and homeostasis of the prostate. The National Cancer Institute (NCI) has estimated that 220,800 men will be diagnosed with and 27,540 men will die of prostate cancer in the USA in 2015 (Ferlay *et al.,* 2010; Howlader *et al.,* 2015). Recently, we reported that AR is one of the attractive targets to treat prostate cancer (PCa) (Elancheran *et al.,* 2015b). Although androgens are often considered to be "male" hormones, they are also found at lower levels in women. Recent studies have found that AR is frequently expressed in primary breast tumors, is estimated to be 50–90 %, depending on the subtypes of breast cancer, and could respond to antiandrogen treatment (Fioretti *et al.,* 2014). Antiandrogens, such as bicalutamide (Chen *et al.*, 2005; Gao *et al.*, 2006), cyproterone acetate (Figg *et al.,* 2010; Neumann and Töpert, 1986), flutamide (Cleve *et al.,* 2011; Brogden and Clissold, 1989) and nilutamide (Hsieh and Ryan, 2008; Moguilewsky *et al.,* 1987; Kassouf *et al.,* 2003) have been used to block the androgen signal, but they have several side effects. Recently, novel AR antagonist, enzalutamide (Scher *et al.,* 2010; Tran *et al.,* 2009), has demonstrated efficacy against castration-resistant prostate cancer (CRPC) and estrogen receptor-negative tumors. Among the subtypes, triple-negative breast cancers (ER-, PR-, HER2-) were positive for AR expression and may respond to treatment with antiandrogen drugs (Ni *et al.,* 2011). ARN-509 (IC50 = 16 nmol/L) binds AR with seven to tenfold greater affinity than the clinically approved antiandrogen, bicalutamide (median IC_{50} = 160 nmol/L), and competes for the same binding site in the ligand-binding pocket of the receptor (Clegg *et al.,* 2012). As a result, there is an

increasing need for the development of new therapy for prostate cancer and breast cancer with better activity profile and less toxicity. Therefore, the concept of non-steroidal, AR antagonists emerged as an attractive target to overcome these problems.

Carbamide ($CO(NH_2)_2$), thiocarbamide ($SC(NH_2)_2$) and sulfonamide (SO_2NH_2) derivatives are the basis of several groups of drugs that have very good biological activities against cancer (Balasubramaninan *et al.,* 2006; Balaji *et al.,* 2014). Oxobenzimidazoles which are highly useful synthetic intermediates have found a myriad of applications in the area of therapeutics (Guo *et al.,* 2012). Oxobenzimidazole analogues were designed by the structural modifications of the three potent structures of the AR antagonist (Fig. 1). Taking into account the interesting properties of these benzimidazole derivatives and in continuation of our research, we designed a series of novel 4-(1-substituted-1,2-dihydro-2-oxobenzo[d]imidazol-3-yl)-2-(trifluoromethyl) benzonitrile using the Schrödinger (Maestro 9.5) software. Since there is no reported full antagonist-bound AR crystal structure, the docking studies were carried out with the available crystal structure of AR bound to steroid agonists such as dihydrotestosterone (DHT) (Jésus-Tran *et al.,* 2006). The compound, 4-(1-allyl-1,2-dihydro-2-oxobenzo [*d*]imidazol-3-yl)-2-(trifluoromethyl) benzonitrile has shown similar binding characters like bicalutamide. In recent years, cesium carbonate has found extensive applications as an excellent base for a variety of synthetic transformations and is superior to other bases in terms of yield, reaction time, reaction temperature and sensitivity toward moisture. Here, we report the design, synthesis and biological evaluation of few 4-(1-substituted-1,2-dihydro-2-oxobenzo[*d*]imidazol-3-yl)-2-(trifluoromethyl) benzonitrile as novel AR antagonists.

Results and discussion

In an attempt to understand the binding mode of our oxobenzimidazole analogues, the ligands (100 compounds) were docked with the crystal structure of the human androgen receptor ligand-binding domain (hARLBD) in complex with dihydrotestosterone agonist (PDB:2AMA) from the Protein Data Bank (Jésus-Tran *et al.,* 2006). To identify molecular determinants responsible for this selectivity, we have taken the crystal structure which contains the hydrophobic, flexible pockets with two deep residues (ARG 752, GLN 711). The metabolic product, DHT, has greater affinity (GS = −10.423 kcal/mol) toward AR which forms hydrogen bonds through the 17β hydroxyl group with two residues (ASN 705, THR 877) in the Helix 12 shown in Fig. 2a, b. The protein was first prepared using the Protein Preparation wizard, and the docking studies were performed using the Schrödinger *Glide* software (*Maestro* 9.5) with extra-precision (XP) mode (Schrödinger, 2013; Friesner *et al.,* 2004; Halgren *et al.,* 2004; Friesner *et al.,* 2006). Out of 100 compounds, we got the appreciable results from the compounds (**9a–n**). The nitrile

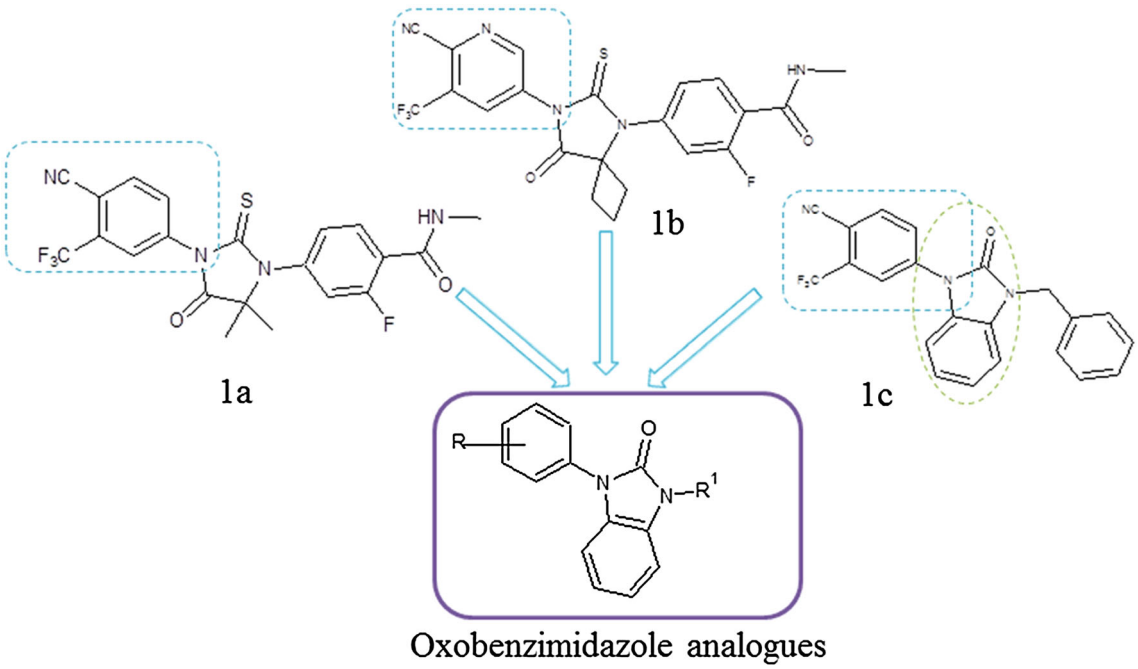

Fig. 1 Three potent structures of AR antagonist discovered to date (**1a**, **1b**, **1c**) together and their structural modifications (Oxobenzimidazole analogues)

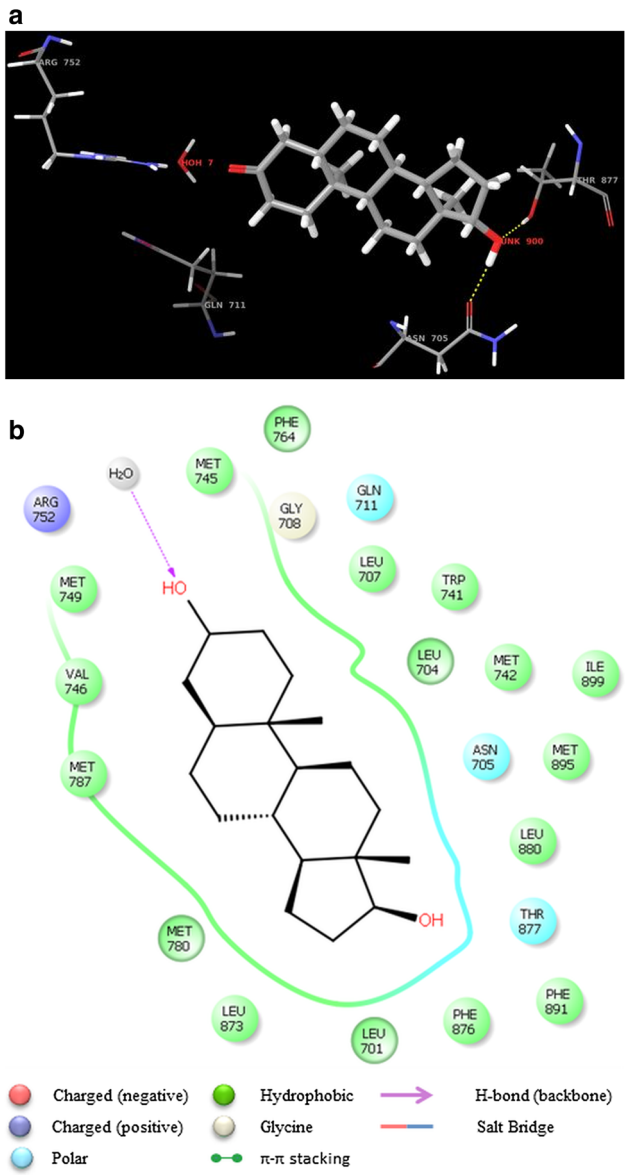

Fig. 2 **a** 3D model of dihydrotestosterone in docking with hARLBD residues in the active site (colored by atom types: C *tan*, N *blue*, O *red*, H *light gray*, F *pink*), **b** 2D diagram interactions of hARLBD with Dihydrotestosterone (Color figure online)

group of the ligand makes the hydrogen bond interactions with ARG752 and GLN711 residues directly and also by way of water-mediated interaction. This pattern of hydrogen bond interaction is similar to that seen with the nitrile group of (*R*)-bicalutamide (Piatnitski Chekler *et al.,* 2014). The Oxobenzimidazole and its N-substituted rings are oriented toward the GLY 708, THR 877, ASN 705 residues to pick up additional hydrophobic interactions. It is interesting to note that the TRP741 residue completely encloses the binding cavity in AR X-ray structures complexes with steroidal agonists such as DHT. Lowest binding energy for the standard and designed ligand-AR (PDB, 2AMA) protein interaction as detected by glide molecular docking is shown in Tables 1 and 2.

Initially, the compounds were designed with the different hydrogen acceptors (CN, Methyl amine, Morpholine) at *para* position and hydrophobic groups (CF3, Cl, F) at *the meta position* (**7a–d**). From the results, we found that CF3 and Cl at *meta* position, CN at *para* positions are essential for getting good glide scores. Further, the compounds extended with the substitution at R^3 showed a better G score compared to the compounds (**7a–d**). The 2D diagram interactions of active AR antagonists (**9a**, **9b**, **9d**, **9f**, **9 m** and **9n**) are shown in Fig. 3. From the docking studies, we found that the compounds (**9a** and **9b)** showed the highest G scores (−9.19 and −9.12 kcal mol^{-1}, respectively) comparatively similar to the standard drug, bicalutamide (−9.94 kcal mol^{-1}). Figure 4 represents the three dimensional model of hARLBD in complex with oxobenzimidazoles.

Based on the molecular docking results, the synthesis of the ligands was considered to be important. The general synthesis of oxobenzimidazoles (**7a**, **7b** and **9a–c)** is depicted in schemes 1 and 2. These compounds were synthesized by prepared bromo substituted benzene, commercially available oxobenzimidazole and allyl or aryl bromide (R^3). The 4-Bromo-2-(substituted) benzonitrile were obtained from 2-(substituted) aniline through the successive bromination (Bartoli *et al.,* 2009) cyanation and diazotization followed by halogenations (Dalton *et al.,* 2008). Oxobenzimidazole coupling with substituted phenyl bromide was affected in the presence of cesium carbonate at N_1 position to afford the requisite N-substituted Oxobenzimidazoles, in low to moderate yield (60–90 %), 8–12 h. The similar reaction was reported by using potassium carbonate, 6 days (Guo *et al.,* 2012). Subsequently, N-alkylation with allyl bromide and 2-Bromo-4′-fluoroacetophenone in the presence of cesium carbonate at N_3 position yielded compounds (**9a–c**).

New compounds, **7a**, **7b** and **9a–c** were well characterized by IR, NMR and HRMS, and all the data are in accordance with the proposed structures. The generation of the heterocyclic structure was confirmed by ^{1}H NMR since the spectra exhibited the characteristic signals of oxobenzimidazole. Indeed, in addition to the signals at δ 4.59 (doublet), δ 5.34 (doublet of doublets) and δ 5.90–5.98 (multiplet) correspond to the N-allyl group. ESI–MS of all compounds showed M+H, M–H or M+K adduct as the molecular ion.

The structure of the compound **9b** was reconfirmed by single-crystal X-ray diffraction method (Sheldrick, 1990, 1997). The Compound **9b** was crystallized under triclinic system with space group P-1. The unit cell parameters of the compound **9b** were as follows: $a = 7.6795(5)$ Å, $b = 9.0374(6)$ Å, $c = 12.9452(9)$ Å, $a = 108.996(4)°$,

Table 1 Lowest binding energy for the Standard ligand-AR (PDB:2AMA) protein interaction as detected by GLIDE molecular docking

ligand	G Score	Lipophilic EvdW	PhobEn	HBond	Electro	Sitemap	LowMW	Penalties	RotPenal
Bicalutamide	−9.94	−6.85	0	−1.11	−0.55	−1.6	−0.07	0	0.23
Andarine	−8.82	−5.71	0	−2.02	−0.76	−0.45	−0.41	0.08	0.45
Bexlosterid	−6.47	−5.04	−0.46	−0.04	−0.1	−0.32	−0.5	0	0
Dutasteride	−6.32	−4.78	−0.41	−0.28	−0.42	−0.4	−0.2	0	0.16
Nilutamide	−5.86	−4.09	0	−0.7	−0.15	−0.59	−0.5	0	0.17
Epristeride	−5.82	−4.79	−0.21	−0.73	0.13	−0.2	−0.17	0	0.16
Flutamide	−5.22	−3.79	0	−0.7	−0.19	−0.28	−0.5	0	0.25

$b = 100.334(4)°$, $g = 98.951(4)°$. Figure 5 represented the ORTEP diagrams of **9b** (Elancheran *et al.,* 2015a).

The human prostate cancer cell lines (PC-3 and LNCaP) and breast cancer cell lines (MCF-7 and MDA-MB-231) were used for the cytotoxicity studies. Cellular viability in the presence and absence of experimental agents was determined using the standard MTT assay as described in the Experimental section (Mosmann, 1983; Rubeinstein *et al.,* 1990; Ishioka *et al.,* 2002; Schayowitz *et al.,* 2008; Khanfar and Sayed, 2010; Khatik *et al.,* 2011; Nunez-Nateras and Castle, 2011). The results of the cytotoxic potential of compounds (**9a–c**, **7a** and **7b**) are listed in Table 3. It is evident that the N-substitution at position, R^3 of the oxobenzimidazole core was influencing the activity in the cell-based assay: N-allyl (**9b**), N-(4-Fluorphenyl) ethanonyl (**9a** and **9c**) displayed similar more active compared to the compounds (**7a** and **7b**). One of the most active compounds of the series, **9b**, contained 4-cyano-3-(trifluoromethyl) phenyl, which is present in many AR ligands. In MTT assays, **9b** was specifically for AR with the IC_{50} values (LNCap: 10.02 ± 0.23 μM and PC-3: 10.91 ± 0.34 μM). In addition, it has evidence that **9b** showed good activity in breast cancer cell lines also. Recent reports depict that antiandrogens are used as a targeted therapy for breast cancer (Niemeier *et al.,* 2010; Garay and Park, 2012).

We have predicted the ADME/T properties of the test compounds (**7a–d** and **9a–n**) and the reference compounds (Nilutamide, Flutamide, Testosterone) for the pharmaceutical relevant properties to assess the drug likeness and pharmacokinetic properties (Jorgensen and Duffy, 2002). The qikpro within *Maestro* 9.5 (Schrödinger, 2013; Friesner *et al.,* 2004, 2006; Halgren *et al.,* 2004) was used for the evaluation of some important absorption, distribution, metabolism and elimination (ADME) parameters and its permissible rangers are listed in Table 4. In the present study, the test compounds showed good drug-like properties based on the logarithm of predicted binding constant to human serum albumin, log KHSA (range for 95 % of drugs: −1.5 to 1.2); the logarithm of predicted blood/brain barrier partition coefficient, log B/B (range for 95 % of drugs: −3.0 to 1.0) the predicted apparent Madin-Darby canine kidney (MDCK) cell permeability in nm s-1 (<25 poor, >500 great); calculated from the predicted Polarizability, QPpolrz, IC_{50} value for blockage of HERG K + channels, log HERG apparent Caco-2 cell permeability, QPP Caco in nm/s, metabolic reactions, #metab, Polarizability, QP polrz.

Conclusion

Thanks to the recent disclosure of the hARLBD X-ray structure, we were able to perform a structure-based design of a novel class of AR antagonists. We designed a series of oxobenzimidazoles using molecular docking, and the glide scores were in good agreement with the observed IC_{50} values. It is evident from the docking calculations that the substitution at R^3 has better binding affinities than the free amide. The compounds (**7a**, **7b** and **9a–c**) were prepared from 2-(substituted) anilines for the cost reduction. The compounds **9a–c** exhibited the significant in vitro cytotoxicity. In particular, compound **9b** was identified as the most promising of the series, especially selective against PC-3 and LNCaP cell lines. The efficacy of the compound (**9b**) against MCF-7 and MDA-MB-231 is also significant, which indicates that AR antagonists may be also used against breast cancer. Further work for this will be continued. We, further, intend to investigate the target site and to study the in vivo anticancer activity of the active compounds.

Experimental section

In silico molecular docking

The protein was first prepared using the Protein Preparation wizard and the docking studies were performed using the Schrödinger *Glide* software within *Maestro* 9.5, which executes the correction of raw PDB structure, where amendments such as the addition of hydrogen atoms,

Table 2 Lowest binding energy for the ligand-AR (PDB:2AMA) protein interaction as detected by GLIDE molecular docking

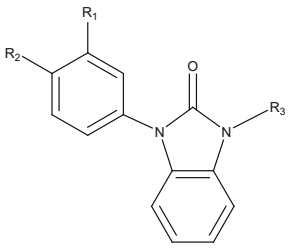

Compd	R^1	R^2	R^3	*G* score	Lipophilic	HBond	Electro
7a	CF_3	CN	H	−6.26	−5.32	0	−0.04
7b	Cl	CN	H	−6.15	−6.88	0	−0.06
7c	F	NH–CH_3	H	−5.22	−3.79	−0.7	−0.19
7d	F	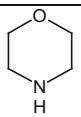	H	−5.05	−5.18	−0.07	−0.08
9a	CF_3	CN	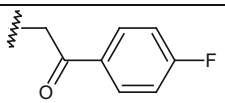	−9.19	−6.91	−0.7	−0.31
9b	CF_3	CN	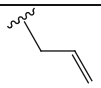	−9.12	−6.35	−1.39	−0.47
9c	Cl	CN	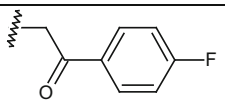	−8.79	−6.33	−1.51	−0.38
9d	Cl	CN	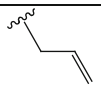	−8.5	−4.85	−0.7	−0.2
9e	CF3	CN	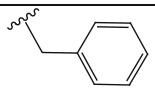	−6.46	−4.91	0	0.02
9f	Cl	CN	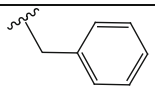	−6.35	−4.89	0	0.02
9g	F	NH–CH_3	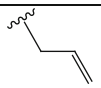	−5.27	−4.33	−0.35	−0.27
9h	F	NH–CH_3	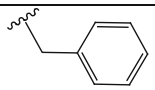	−5.09	−4.16	−0.35	−0.27
9i	F	NH–CH_3	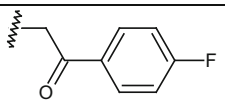	−5.49	−4.56	0	−0.03
9j	F	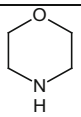	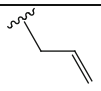	−7.99	−6.82	0	−0.09

Table 2 continued

9k	F		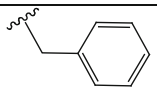	−7.82	−7.23	−0.47	−0.11
9l	F		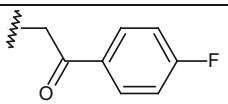	−7.64	−4.83	−0.72	−0.37
9m	H	CN	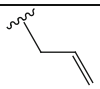	−6.4	−6.35	0	−0.23
9n	H	CN	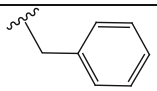	−6.36	−4.96	−0.7	−0.41

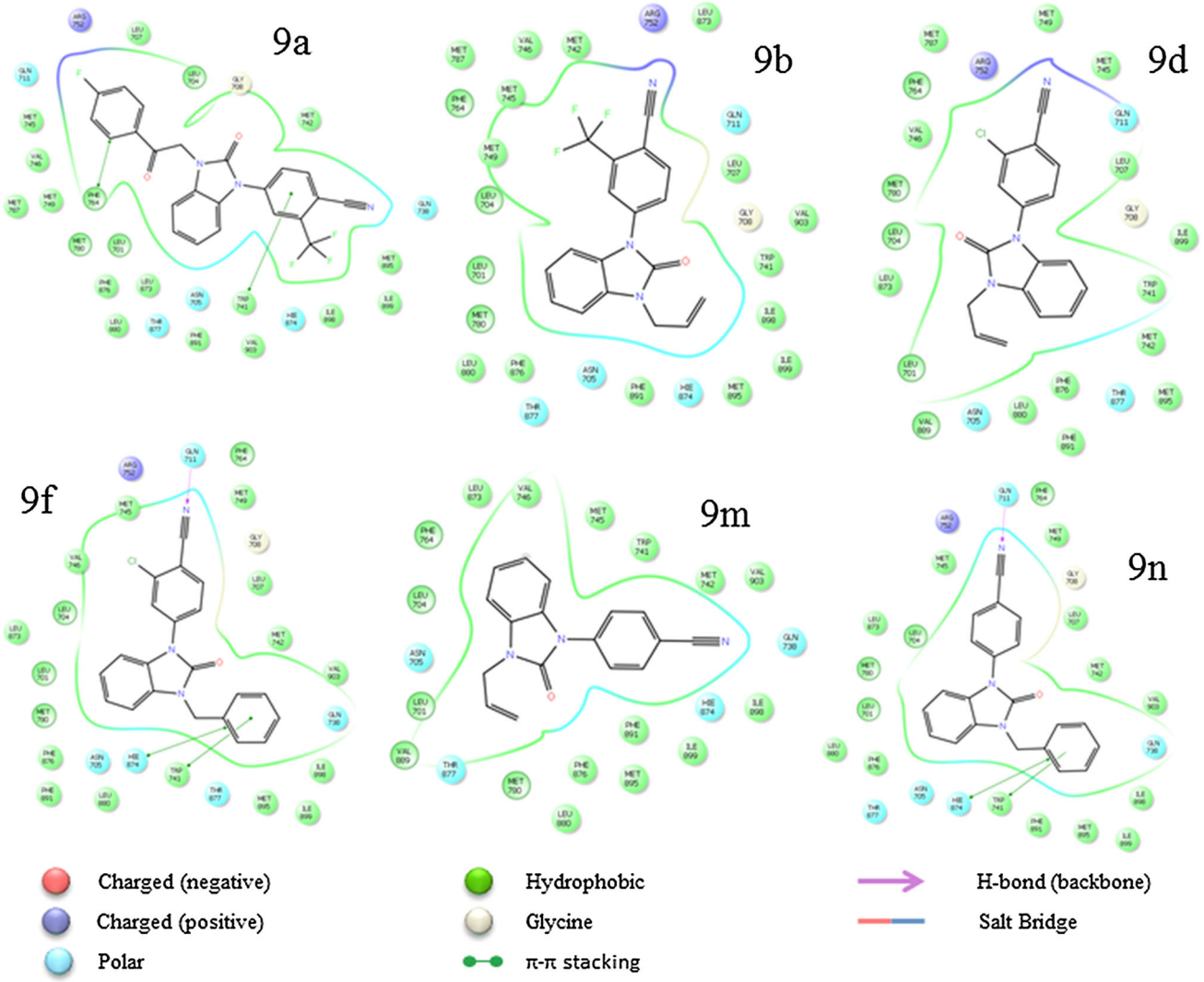

Fig. 3 2D diagram interactions of active AR antagonists (**9a**, **9b**, **9d**, **9f**, **9m**, **9n**)

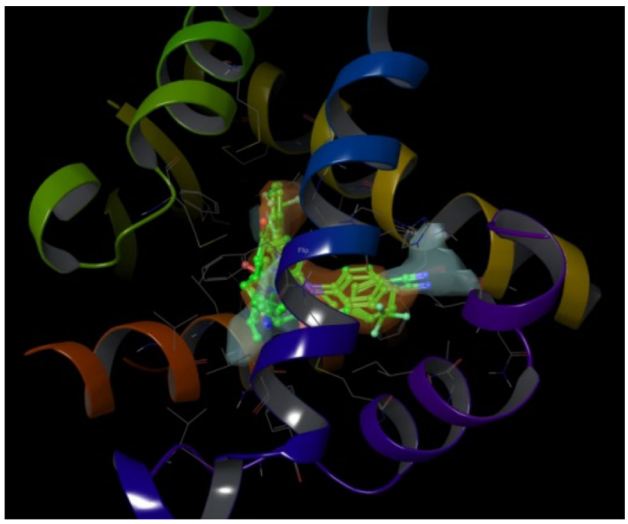

Fig. 4 Three-dimensional model of oxobenzimidazoles in the AR-binding site (colored by atom types: C *green*, N *blue*, O *red*, S *yellow*, H *light gray*) (Color figure online)

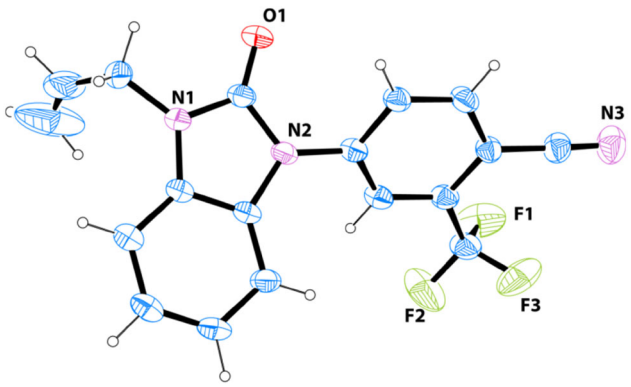

Fig. 5 ORTEP representation of the compound **9b**

assigning bond orders, creating disulfide bonds, fixing of the charges and orientation of groups were incorporated. Ligand preparation was performed using LigPrep for the corrections on the ligands such as the addition of hydrogens, 2D to 3D conversion, bond lengths and bond angles, low energy structure, and ring conformation followed by minimization and optimization in optimized potential for liquid simulations (OPLS, 2005) force field. *Glide* is a ligand docking program for predicting protein–ligand binding modes and ranking ligands via high-throughput virtual screening. *Glide* molecular docking needs an X-ray crystal structure of protein binding with ligands for determining active site receptor grid. Receptor grid-based molecular docking assists the ligands to bind in more than one possible conformation. *Glide* searches for favorable interactions between one or more ligand molecules and a protein. The van der Waals radii of the receptor atoms with partial atomic charges are to be less than the specified cutoff. The scaling factor and partial charge cutoff are 1 and 0.25 Å, respectively. The G score is calculated in kcal/mol, and it includes ligand–protein interaction energies, hydrophobic interactions, hydrogen bonds, internal energy, π–π stacking interactions, and root mean square deviation (RMSD) and desolvation. Glide utilizes two different scoring functions, SP and XP Glide Score, to rank-order compounds. *Glide* module of the XP visualizer

Scheme 1 Synthesis of compounds **5a** and **5b**. Reagents and conditions: **a** N-Bromosuccinimide, DMF, RT, **b** CuCN, DMF, reflux, **c** $NaNO_2$, CuBr, Conc.HCl, 0 °C to RT

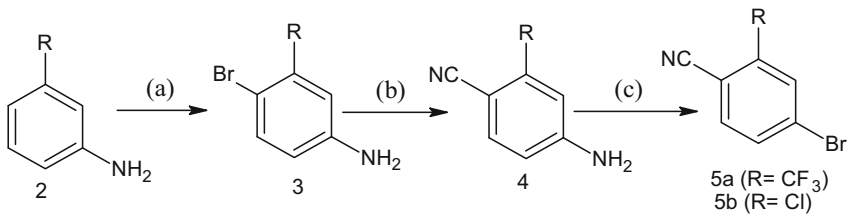

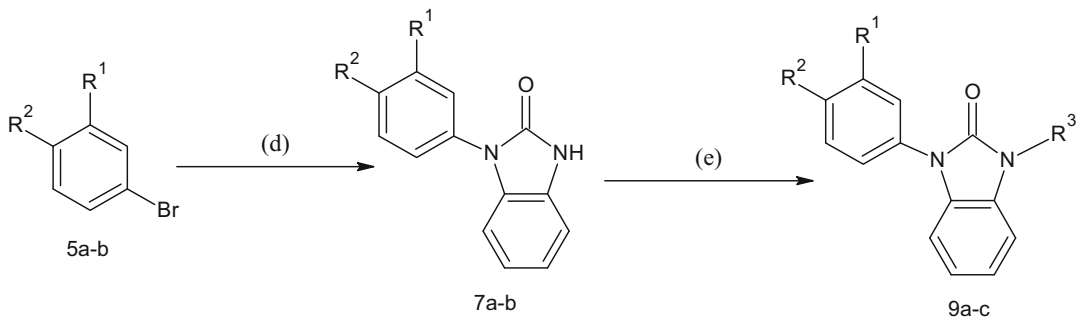

Scheme 2 Synthesis of compound **7a**, **b**, **9a–c**. Reagents and conditions: (*d*) 2-hydroxy benzimidazole (6), Cs_2CO_3, DMF, 110 °C (*e*) R-X (8), Cs_2CO_3, DMF, 110 °C

Table 3 Cytotoxicity studies expressed by IC_{50} in μM for compounds **9a–c**, **7a** and **7b** and for the positive controls, bicalutamide and doxorubicin

Compounds	IC_{50} (μM) on LNCaP[a]	IC_{50} (μM) on PC-3[a]	IC_{50} (μM) on MCF-7[a]	IC_{50} (μM) on MDA-MB-231[a]
9a	11.2 ± 0.13	12.19 ± 0.25	20.2 ± 0.73	26.2 ± 0.13
9b	10.02 ± 0.23	10.91 ± 0.34	15.6 ± 0.82	22.25 ± 0.25
9c	20.56 ± 0.19	15.71 ± 0.52	25.61 ± 0.95	52.3 ± 0.62
7a	50.91 ± 0.85	45.21 ± 0.92	>100	>100
7b	65.54 ± 2.1	55.23 ± 0.56	>100	>100
Bicalutamide[b]	1.71 ± 0.12	77	nd[c]	nd[c]
Doxorubicin[b]	nd[c]	nd[c]	0.36 ± 0.03	0.20 ± 0.01

[a] The values are the mean ± standard deviation (SD) of three independent experiments performed in triplicate

[b] Positive control

[c] *nd* not determined

analyzes the specific ligand–protein interactions. Grids were generated using *Glide* version 9.5 following the standard procedure recommended by Schrodinger.

Chemistry

General

All reagents and solvents were purchased from Sigma-Aldrich, Spectrochem and Merck Scientific, and used without further purification unless otherwise stated. Melting points were recorded on a Buchi Melting Point M-565 system. All the reaction mixtures and column eluents were monitored by thin-layer chromatography (TLC) on Merck silica gel 60 F254 pre-coated aluminum plates with a thickness of 0.2 mm and were developed with the mixtures of hexane/ethyl acetate or CH_2Cl_2/Methanol and were visualized with UV light at 254 and 365 nm. Column chromatography was performed under "flash" conditions on Merck silica gel (230–400 mesh). Infrared spectra (IR) were recorded using KBr discs, γ (cm^{-1}), on a Thermo Scientific IR spectrophotometer. Accurate masses (HRMS) were determined using a Thermo Scientific Exactive plus LC–MS/MS mass spectrometer. ^1H and ^{13}C NMR spectra were recorded in $CDCl_3$ or DMSO-d6 using a Bruker 400 MHz NMR instrument. Chemical shifts are given in δ values (ppm) using tetramethylsilane as the internal standard. Peak multiplicities are expressed as follows: s, singlet; d, doublet; t, triplet; q, quartet; dd, doublet of doublet; br, broad; br s, broad singlet; m, multiplet.

*General procedure for the synthesis of 4-Bromo-3-(substituted) aniline (**3a–b**)*

To a solution of substituted aniline **2a** or **2b** in DMF 100 ml was added to a solution of NBS (92 mmol, 1.0 eq) in DMF 100 ml dropwise. The reaction mixture was stirred at room temperature for 3 h, then diluted with ethyl acetate 500 ml and washed with brine 2 × 150 ml. The organic phase was dried Na_2SO_4, filtered and concentrated to give the title compound **3a** or **3b** as brownish solid, 90–92 % yield. To a solution of **2a** or **2b** (0.8 mmol) in the selected solvent (1 ml), a solution of NBS (0.8 mmol) in the same solvent (1 ml) was added batch wise at room temperature, and the reaction was monitored by LC–MS/MS. Mixtures were obtained with traces of dibrominated products.

*4-Bromo-3-(trifluoromethyl) aniline (**3a**)* Yield: 92 %; mp 48–50 °C; brownish powder; IR (KBr) ν max: 3485–3362 ($N–H_{stretch}$), 2219 ($C\equiv N$), 1627 ($N–H_{bend}$), 1615 1566, 1509, 1467 ($C=C_{arom}$), 1361, 1185, 1121, 1044 ($C–H_{bend}$), 1276, 550 (CF3) cm^{-1}; ^1H NMR (CDCl3, 400 MHz, ppm): δ 7.38 (d, 1H, $J = 8.8$ Hz, C5-H), 6.95 (d, 1H, $J = 2.8$ Hz, C2–H), 6.63 (dd, 1H, $J = 2$ Hz, $J =$ 8.4 Hz, C6-H), 3.84 (br s, 2H, $–NH_2$); ^{13}C NMR (100 MHz, $CDCl_3$, ppm): δ 145.7 (C1),135.5 (C5), 130.6 (C3), 124.3 (C6), 121.6 (CF3), 119.07 (C2), 114.1 (C4); HRMS (ESI): *m/z* calculated for $C_7H_5^{79}BrF_3N$ $[M–H]^-$: 237.94847; Found: 237.94478; Calculated for $C_7H_5^{81}BrF_3N$ $[M–H]^-$: 239.94620; Found: 239. 94250.

*4-Bromo-3-chloro aniline (**3b**)* Yield: 90 %; mp 63–64 °C; brownish Powder; IR (KBr) ν max: 3486, 3371 ($N–H_{stretch}$), 2224 ($C\equiv N$), 1627 ($N–H_{bend}$), 1605, 1547, 1506 ($C=C_{arom}$), 1333, 1253, 1152, 1040 ($C–H_{bend}$), 823, 713 ($C–Cl_{bend}$) cm^{-1}; ^1H NMR (CDCl3, 400 MHz, ppm): δ 7.33 (d, $J = 8.67$ Hz, 1H, C5-H), 6.79 (d, $J = 2.64$ Hz, 1H, C2-H), 6.45 (dd, $J = 8.67$, 2.64 Hz, 1H, C6-H), 3.74 (broad s, 2H, −NH2); ^{13}C NMR (100 MHz, $CDCl_3$, ppm): δ 146.7 (C1),134.6 (C3), 133.9 (C5), 116.4 (C6), 115.1 (C2), 109.8 (C4); HRMS (ESI): *m/z* Calcd for $C_6H_5^{79}Br^{35}ClN$ $[M+H]^+$: 205.93667; Found: 205.93427; Calcd

Table 4 Evaluation of drug-like properties of the lead molecules by Qikpro Maestro 9.5 molecular docking suite

S.No	Ligands	Molecular weight	Donor HB	Accept HB	Q log Po/w (−2.0 to 6.5)	QP log HERG (concern <−5)	QPP Caco	#metab	QP polrz	QP log BB	QPPMDCK	QP log Khsa	QP log Kp	Percent Human Oral Absorption
1	7a	303.243	1	3.5	2.934	−5.114	428.214	1	30.239	−0.549	740.429	0.255	−3.149	91.224
2	7b	269.686	1	3.5	2.452	−5.114	380.347	0	28.42	−0.685	389.785	0.127	−3.2	87.484
3	7c	257.263	2	3	2.671	−5.018	1082.503	2	28.385	−0.306	915.141	0.151	−2.382	96.898
4	7d	313.326	1	4.7	3.048	−4.856	1614.068	1	33.673	−0.094	1265.656	0.279	−2.204	100
5	9a	439.368	0	5.5	4.857	−6.705	617.773	2	44.608	−0.638	1993.064	0.57	−2.079	100
6	9b	343.308	0	3.5	4.286	−0.322	1114.7	2	35.453	−0.322	2083.738	0.518	−2.09	100
7	9c	405.815	0	5.5	4.369	−6.724	548.691	1	42.835	−0.784	1048.637	0.431	−2.126	100
8	9d	309.754	0	3.5	3.799	−5.593	990.097	1	33.682	−0.467	1096.597	0.379	−2.137	100
9	9e	393.361	0	3.5	4.852	−5.538	1028.563	1	39.523	−0.432	1582.341	0.451	−1.652	100
10	9f	359.814	0	3.5	4.845	−6.529	1058.621	1	40.295	−0.478	1178.961	0.763	−1.592	100
11	9g	297.331	1	3	4.225	−5.5	2817.929	3	33.648	−0.063	2574.119	0.567	−1.318	100
12	9h	347.391	1	3	5.24	−6.475	2949.216	3	40.257	−0.069	2704.002	0.928	−0.797	100
13	9i	393.392	1	5	4.893	−6.646	1560.149	3	42.836	−0.34	2459.049	0.711	−1.306	100
14	9j	353.395	0	4.7	4.349	−5.372	4452.576	2	38.996	0.179	3790.314	0.463	−1.081	100
15	9k	403.455	0	4.7	5.363	−6.326	4477.874	2	45.525	0.165	3813.641	0.843	−0.601	100
16	9l	449.456	0	6.7	4.892	−6.532	2328.404	2	48.087	−0.108	3404.171	0.512	−1.13	100
17	9m	275.309	0	3.5	3.311	−5.7	905.886	1	32.455	−0.649	444.581	0.262	−2.069	100
18	9n	325.369	0	3.5	4.352	−6.628	965.277	1	39.044	−0.663	476.169	0.645	−1.529	100
19	Nilutamide	317.224	1	4.5	2.143	−4.234	224.432	2	28.728	−0.815	359.233	0.086	−4.319	61.71
20	Flutamide	276.215	1	3.5	2.683	−4.543	776.369	3	25.871	−0.452	1394.807	0.062	−3.011	76.611
21	Testosterone	288.429	1	3.7	3.133	−3.227	1198.919	3	31.88	−0.286	601.884	0.495	−3.103	76.554

the predicted IC_{50} value for blockage of HERG K+ channels, log HERG (concern < −5); the predicted apparent Caco-2 cell permeability, QPP Caco in nm/s.(<25 poor, >500 great); the number of likely metabolic reactions, #metab (range for 95 % of drugs: 1–8); the predicted Polarizability, QP polrz (13.0–70.0 for 95 % of drugs); the logarithm of predicted blood/brain barrier partition coefficient, log B/B (range for 95 % of drugs: −3.0 to 1.0); the predicted apparent Madin-Darby canine kidney (MDCK) cell permeability, QPPMDCK in nm s^{-1} (<25 poor, >500 great); the logarithm of predicted binding constant to human serum albumin, log KHSA (range for 95 % of drugs: −1.5 to 1.2); and the predicted skin permeability, log Kp (−8.0 to −1.0 for 95 % of drugs)

for $C_6H_5^{79}Br^{35}ClN$ $[M+H]^+$: 207.93396; Found: 207.93156.

*General procedure for the synthesis of 4-cyano-3-(substituted) aniline (**4a, b**)*

A mixture of compound **3a** or **3b** (19 mmol) and CuCN (29 mmol, 1.5 eq) in DMF (20 ml) was heated at 145 °C under nitrogen overnight. The reaction mixture was cooled to room temperature and then poured into ice water (50 ml). Ethyl acetate (100 ml) was added and the insoluble solid was filtered off (washed with ethyl acetate [2 × 30 ml]). The organic layer was separated, and the aqueous layer was extracted with ethyl acetate (2 × 50 ml). The combined extracts were washed with saturated aqueous $NaHCO_3$ solution (1 × 150 ml), brine (3 × 100 ml) and dried over Na_2SO_4. The resulting material was concentrated and the residue was purified by silica gel chromatography (petroleum ether:ethyl acetate, 10:1) to afford the title compound (**4a** or **4b**) as a gray solid (60–65 % yield).

*4-Amino-2-(trifluoromethyl) benzonitrile (**4a**)* Yield: 65 %; mp 143–145 °C, Gray Powder; IR (KBr) ν max: 3485–3362 ($N–H_{stretch}$), 2219 ($C\equiv N$), 1627 ($N–H_{bend}$), 1615 1566, 1509, 1467 ($C=C_{aroma}$), 1361, 1185, 1121, 1044 ($C–H_{bend}$), 1276, 550 (CF3) cm^{-1}; ^1H NMR ($CDCl_3$, 400 MHz, ppm): δ 7.46 (d, $J = 3.6$ Hz, 1H, C6-H), 7.01 (d, $J = 2$ Hz, 1H, C3-H), 6.82 (dd, $J = 2.4$ Hz, $J = 5.2$ Hz, 1H, C5-H), 6.12 (br s, 2H, –NH2); ^{13}C NMR (100 MHz, $CDCl_3$, ppm): δ 152.6 (C4), 135.1 (C6), 132.7 (C2), 123.3 (C5), 120.5 (CF3), 116.7 (C3), 114.9 (CN), 110.7 (C1); HRMS (ESI): *m/z* calculated for $C_8H_5F_3N_2$ $[M–H]^-$: 185.03321; Found: 185.03133.

*4-Amino-2-chlorobenzonitrile (**4b**)* Yield: 60 %; mp 116–118 °C, Gray powder; IR (KBr) ν max: 3486, 3371 ($N–H_{stretch}$), 2224 ($C\equiv N$), 1627 ($N–H_{bend}$), 1605, 1547, 1506 ($C=C_{arom}$), 1333, 1253, 1152, 1040 ($C–H_{bend}$), 823, 713 ($C–Cl_{bend}$) cm^{-1}; ^1H NMR (CDCl3, 400 MHz, ppm): δ 7.32 (d, $J = 8.4$ Hz, 1H, C6-H), 6.64 (d, 1H, C3-H), 6.47(d, $J = 8.4$ Hz, 1H, C5-H), 4.23 (br s, 2H); ^{13}C NMR (100 MHz, $CDCl_3$, ppm): δ 150.3 (C4), 137.1 (C2), 134.0 (C6), 116.3 (C5), 113.7 (C3), 111.8 (CN), 99.9 (C1); HRMS (ESI): *m/z* calculated for $C_7H_5ClN_2$ $[M+H]^+$: 153.02140; Found: 153.02168.

*General procedure for the synthesis of 4-Bromo-2-(substituted) benzonitrile (**5a, b**)*

4-Cyano-3-(substituted) aniline **4a** or **4b** (38 mmol) was dissolved in conc. HCl (27 ml). After cooling to 0 °C, sodium nitrite (39 mmol, 1.5 eq) was added very slowly to the stirred solution with the temperature being kept within (0 and 5 °C). This diazonium salt solution was then poured into a flask containing CuBr (53 mmol, 1.4 eq) and 22 ml of conc. HCl. The solution was stirred for 2 h, and then, the reaction mixture was poured into ice water (50 ml) extracted with Ethyl acetate (100 ml). The organic layer was separated, and the aqueous layer was extracted with ethyl acetate (2 × 50 ml). The combined extracts were washed with saturated aqueous $NaHCO_3$ solution (1 × 150 ml), brine (3 × 100 ml) and dried over Na_2SO_4. The resulting material was concentrated, and the residue was purified by silica gel chromatography (petroleum ether:ethyl acetate, 10:1) to afford the title compound (**5a** or **5b**) as white solid (72–75 % yield).

*4-Bromo-2-(trifluoromethyl) benzonitrile (**5a**)* Yield 75 %; White Solid; IR (KBr) ν max: 3101, 3040 ($C–H_{arom}$), 2924, 2853 ($C–H_{alk}$), 2235 ($C\equiv N$), 1594, 1558, 1542, 1508, 1484, 1405 ($C=C_{arom}$), 1182, 1142, 1057 ($C–H_{bend}$), 1304, 1270, 551 (C–CF3) cm^{-1}; ^1H NMR (400 MHz, $CDCl_3$, ppm): δ 7.96 (s, 1H, H-2), δ 7.87 (d, $J = 8.0$ Hz, 1H, H-6), 7.74 (d, $J = 8.0$ Hz, 1H, H-5); ^{13}C NMR (100 MHz, $CDCl_3$, ppm): δ 135.8 (C6), 134.4, 133.8 (q, $J = 65.5$ Hz, C2), 130.3 (q, CF3), 128.2 (d, $J = 26$ Hz, C5), 122.9 (C3), 120.2 (C4), 114.8 (CN), 108.9 (C1); HRMS (ESI): *m/z* Calcd for $C_8H_3^{79}BrF_3N$ $[M+H]^+$: 249.94737 Found: 249.94696; Calcd for $C_8H_3^{81}BrF_3N$ $[M+H]^+$: 251.94520; Found: 251.94479.

*4-Bromo-2-chlorobenzonitrile (**5b**)* Yield 72 %; White Solid; IR (KBr) ν max: 3083 ($C–H_{arom}$), 2937, 2835 ($C–H_{alk}$), 2233 ($C\equiv N$), 1579, 1548, 1542, 1467 ($C=C_{arom}$), 1182, 1151, 1117 ($C–H_{bend}$), 830, 692 ($C–Cl_{bend}$) cm^{-1}; ^1H NMR (400 MHz, $CDCl_3$, ppm): δ 7.71 (s, 1H, H-2), 7.55 (d, $J = 1.2$ Hz, 2H, H-5, H-6); ^{13}C NMR (100 MHz, $CDCl_3$, ppm): δ 134.8 (C6), 127.8 (C2), 126.5 (C5), 123.7 (C3), 123.3 (C4), 110.3 (CN), 109.2 (C1); HRMS (ESI): *m/z* Calcd for $C_7H_3^{79}Br^{35}ClN$ $[M+K]^+$: 255.4624 Found: 255.96956; Calcd for $C_7H_3^{79}Br^{37}ClN$ $[M+K]^+$: 257.4624; Found: 257.96722.

*General procedure for the synthesis of compounds (**7a, b**)*

4-Bromo-2-(substituted) benzonitrile **5a** or **5b** (5 mmol) was added to a mixture of 1*H*-benzo[d]imidazol-2(3*H*)-one (**6**) (10 mmol) and Cs_2CO_3 (10 mmol) in DMF (25.0 ml). After 12 h, 50 ml of ice water was added dropwise. The resulting suspension was filtered, and the filter cake was dried in a vacuum oven. The solid was purified by flash chromatography (50 % ethyl acetate in hexane) to afford 4-(2-oxo-2,3-dihydro-1*H*-benzo[d]imidazol-1-yl)-2-(substituted) benzonitrile (**7a** or **7b**).

*2-(Trifluoromethyl)-4-(1,2-dihydro-2-oxobenzo[d]imidazol-3-yl) benzonitrile (**7a**)* Yield 62 %; White Solid; mp 232–233 °C; IR (KBr) ν max: 3189, 3149 (N–$H_{stretch}$), 3072 (C–H_{arom}), 2957, 2895, 2820 (C–H_{alk}), 2230 (C≡N), 1720 (C=O), 1611 (N–H_{bend}), 1575, 1507, 1481, 1439 (C=C_{arom}), 1385, 1319, 1240, 1185, 1127, 1053 (C–H_{bend}), 1272, 558 (C–CF3) cm^{-1}; ^1H NMR (400 MHz, $CDCl_3$, ppm): δ 9.372 (s, 1H, NH), 8.14 (s, 1H, H-2), 8.03 (d, 2H, H-5,H-6), 7.2 (m, 4H, phenyl); ^{13}C NMR (100 MHz, $CDCl_3$, ppm): δ 152.9 (C=O), 139.2 (C4), 135.6 (C6), 133.8, 133.1 (q, $J = 65$ Hz, C2), 128.5 (C′ 1), 127.6 (d, $J = 34$ Hz, C5), 123.3 (C′ 6), 122.8 (C′ 3), 122.5 (q, CF3), 121.6 (C), 120.4 (C′ 5), 114.8 (CN), 110.0 (C′ 2), 108.7 (C′ 4), 106.6 (C1); HRMS (ESI): *m/z* calculated for $C_{15}H_8F_3N_3O$ $[M+H]^+$: 304.06922; Found: 304.069.

*2-(Chloro)-4-(1,2-dihydro-2-oxobenzo[d]imidazol-3-yl) benzonitrile (**7b**)* Yield 62 %; White Solid; mp 225–226 °C; IR (KBr) ν max: 3188, 3150(N–$H_{stretch}$), 3076 (C–H_{arom}), 2924, 2853 (C–H_{alkane}), 2230 (C≡N), 1719 (C=O), 1611 (N–H_{bend}), 1575, 1510, 1481, 1438 (C=C_{arom}), 1387, 1319, 1240, 1195, 1127, 1053 (C–H_{bend}), 830, 701 (C–Cl_{bend}) cm^{-1}; ^1H NMR (400 MHz, $CDCl_3$, ppm): δ 8.17 (s, 1H), 8.01 (d, 2H), 7.39 (m, 4H); ^{13}C NMR (100 MHz, $CDCl_3$, ppm): δ 152.3 (C=O), 139.4 (C4), 136.4 (C2), 134.5 (C′ 1), 133.9 (C6), 123.3 (C′ 6), 122.9 (C′ 3), 122.2 (C′ 5), 119.5 (C′ 2), 117.6 (C5), 116.2 (C′ 4), 115.1 (C3), 114.2 (CN), 109.1 (C), 105.2 (C1); HRMS (ESI): *m/z* calculated for $C_{14}H_8ClN_3O$ $[M-H]^-$: 268.02831; Found: 268.02609.

*General procedure for the synthesis of compounds (**9a–c**)*

2-(Substituted)-4-(1,2-dihydro-2-oxobenzo[d]imidazol-3-yl) benzonitrile **7a** or **7b** (5 mmol) was added to a mixture of compound (R–X) and Cs_2CO_3 (10 mmol) in DMF (25.0 ml). After 12 h, 50 ml of ice water was added dropwise. The resulting suspension was filtered, and the filter cake was dried in a vacuum oven. The solid was purified by flash chromatography (50 % ethyl acetate in hexane) to afford the title compound (**9a–c**).

*4-{3-[2-(4-Fluorophenyl)-2-oxoethyl]-2-oxo-2,3-dihydro-1H-benzimidazol-1-yl}-2-(trifluoromethyl) benzonitrile (**9a**)* Yield 80 %; Colorless needles; mp 178–180 °C; IR (KBr) ν max: 3063 (C–H_{arom}), 2954, 2916, 2851 (C–H_{alkane}), 2236 (C≡N), 1712, 1696 (2 C=O), 1602, 1508, 1489, 1437 (C=$C_{aromatic}$), 1365, 1347, 1312, 1240, 1180, 1161, 1135, 1055 (C–H_{bend}), 1276, 550 (C–CF3) cm^{-1}; ^1H NMR (400 MHz, $CDCl_3$, ppm): δ 8.23(s, 1H, H-2), 8.03 (s, 4H, phenyl), 7.19–7.23 (m, 2H, H-5, H-6), 7.09–7.13 (m, 4H, phenyl), 3.72 (s, 2 H, –CH2–CO); ^{13}C NMR (100 MHz, $CDCl_3$, ppm): δ 193.5 (C=O), 157.2 (C″ 4), 153.3 (N–C=O), 138.3 (C4), 136.5 (C′ 1), 135.6 (C6), 134.2, 133.6 (q, $J = 60$ Hz, C2), 133.2 (C″ 1), 130.6 (C″ 2, C″ 6), 129.1 (C′ 6), 127.6 (d, $J = 34$ Hz, C5), 125.6 (C′ 3), 124.0 (C′ 5), 122.8, 122.5 (q, CF3), 120.6 (C′ 2), 118.8 (C′ 4), 115.6 (C″ 3, C″ 5), 115.8 (C3), 114.2 (CN), 102.3 (C1), 44.9 (CH2); HRMS (ESI): *m/z* calculated $C_{23}H_{13}F_4N_3O_2$ $[M-H]^-$: 438.08711; Found: 438.087.

*4-(1-Allyl-1,2-dihydro-2-oxobenzo[d]imidazol-3-yl)-2-(trifluoromethyl) benzonitrile (**9b**)* Yield 85 %; Colorless needles; mp 107–108 °C; IR (KBr) ν max: 3070 (C–H_{arom}), 2925, 2853 (C–H_{alk}), 2232 (C≡N), 1709 (C=O), 1607, 1572, 1506, 1489, 1435, 1400 (C=C_{arom}), 1347, 1308, 1280, 1225, 1177, 1146, 1132, 1052 (C–H_{bend}), 1280, 557 (C–CF3) cm^{-1}; ^1H NMR (400 MHz, $CDCl_3$, ppm): δ 8.15(s, 1H, H-2), 8.01 (d, $J = 1.2$ Hz, 2H, H-5, H-6), 7.06–7.27 (m, 4H, phenyl), 5.90–5.98 (m, 1H,CH), 5.34 (dd, $J = 5.6$ Hz, 2 H, = CH2), 4.59 (d, $J = 5.2$ Hz, 2 H, –CH2–); ^{13}C NMR (100 MHz, $CDCl_3$, ppm): δ 152.3 (C=O), 139.4 (C4), 136.0 (C6), 134.7, 134.0 (q, $J = 66$ Hz, C2), 132.1(C′ 1), 131.2(C′ 6), 129.5(C′ 3), 127.3(C″ 2), 123.5, 123.0 (q, CF3), 123.0(d, C5), 122.2(C′ 5), 121.3(C′ 2),120.6 (C3), 118.5 (C′ 4), 117.6 (C″ 3), 115.1(CN), 108.0 (C1), 43.7 (C″ 1); HRMS (ESI): *m/z* calculated for $C_{18}H_{12}F_3N_3O$ $[M+H]^+$: 344.10052; Found: 344.0986.

*2-Chloro-4-{3-[2-(4-fluorophenyl)-2-oxoethyl]-2-oxo-2,3-dihydro-1H-benzimidazol-1-yl}benzonitrile (**9c**)* Yield 82 %; White Solid; mp 175–176 °C; IR (KBr) ν max: 3072 (C–H_{arom}), 2925, 2852 (C–H_{alk}), 2229 (C≡N), 1720, 1693 (2 C=O), 1602, 1510, 1484, 1437 (C=C_{arom}), 1382, 1330, 1240, 1195, 1130, 1054 (C–H_{bend}), 829, 695 (C–Cl_{bend}) cm^{-1}; ^1H NMR (400 MHz, $CDCl_3$, ppm): δ 3.7 (s, 2 H, –CH2) 7.09–7.13 (m, 4H,), δ 7.13–7.16 (m, 4H, phenyl), 7.37–7.41 (m, 2H, H-5, H-6), 8.01 (s, 4H, phenyl) 8.28 (s, 1H, H-2); ^{13}C NMR (100 MHz, $CDCl_3$, ppm): δ 192.05 (C=O), 157.2 (C″ 4), 152.3 (N–C=O), 139.4 (C4), 136.4 (C2), 134.5 (C′ 1), 133.9 (C6), 131.7(C″ 1), 130.5 (C″ 2, C″ 6), 127.3 (C′ 6), 123.5 (C′ 3), 122.7 (C′ 5), 119.5 (C′ 2), 118.2 (C5), 116.5 (C′ 4), 115.6 (C″ 3, C″ 5), 115.1 (C3), 114.0 (CN), 109.1 (C), 104.2 (C1), 44.1 (CH2); HRMS (ESI): *m/z* calculated for $C_{22}H_{13}ClFN_3O_2$ $[M+H]^+$: 406.8089; Found: 406.9141.

X-ray diffraction analysis

The single crystal of the compound was developed by slow evaporation of chloroform and alcohol (1:1 ratio). The XRD data for a good-quality single crystal ($0.40 \times 0.34 \times 0.22$ mm^3) was collected at 296 K temperature with a Bruker 3-circle diffractometer (Bruker Nonius SMART APEX 2) equipped with CCD area detector. Bruker SMART software was used for data collection and also for indexing reflections and unit cell

parameters. The data were integrated using SAINT software. The structure was solved by direct methods and refined by full-matrix least squares calculation using SHELXL software. Lattice parameters were determined from θ values in the range $1.72 < \theta < 24.50$.

In vitro cytotoxicity evaluation

Cell lines and cell culture

Human prostate cancer cell lines, PC-3 and LNCaP and breast cancer cell lines, MCF-7 and MDA-MB-231 were obtained from National Centre for Cell Science (NCCS), Pune, India, and were cultured in RPMI1640 and DMEM, respectively, with 10 % fetal bovine serum (FBS), MTT, EDTA, trypsin and 1 % penicillin–streptomycin. DMEM, RPMI1640, FBS, 1 % penicillin–streptomycin, bicalutamide and dextrorubicin were purchased from Sigma-Aldrich. Cell cultures were maintained in flasks under standard conditions: incubation at 37 °C and 5 % CO_2. All the subcultures were used prior to passage 15. Cells were routinely passaged using 0.25 % trypsin/0.1 % EDTA. For treatment, cells were cultured in the presence of increasing concentrations (1–100 μM) of compounds for 24 h.

In vitro cytotoxicity measurements

All in vitro experiments for cell proliferation/inhibition were performed in triplicates. For the PC-3 cell growth inhibition assay, cells were cultured in RPMI1640 supplement and trypsinized, further diluted to 2.0×10^4 cell/ml with RPMI1640 supplemented with 10 % fetal bovine serum. This cell suspension was transferred to 96-well microtiter plates, and incubated in the presence or absence of increasing concentration of positive control (Bicalutamide) or the test compounds (1–100 μM) at 37 °C and 5 % CO_2. After 24-h incubation, cells were treated with an MTT solution for 4 h in a cell culture incubator at 37 °C and 5 % CO_2. Cell proliferation was determined by the MTT method. MTT which is a tetrazolium salt is converted into insoluble formazan by mitochondrial dehydrogenases in live cells. Formazan is dissolved in DMSO (Merck), and absorbance was measured at dual wavelength of 550 and 630 nm on a Varioskan™ Flash Multimode Reader (Thermo Scientific Instrument). Similar experiments were performed in LNCaP, MCF-7 and MDA-MB-231 cells also.

ADME property studies

A set of ADMET-related properties of the ligands were calculated by using the QikProp which generates physically relevant descriptors and uses them to perform ADMET predictions. The methods implemented were developed by Jorgensen and Duffy, the logarithm of aqueous solubility, log Swat (range for 95 % of drugs: −6.0 to 0.5); the logarithm of predicted binding constant to human serum albumin, log KHSA (range for 95 % of drugs: −1.5 to 1.2); the logarithm of predicted blood/brain barrier partition coefficient, log B/B (range for 95 % of drugs: −3.0 to 1.0) the predicted apparent Madin-Darby canine kidney (MDCK) cell permeability in nm s^{-1} (<25 poor, >500 great); the index of cohesion interaction in solids, Indcoh, calculated from the predicted Polarizability, QPpolrz, IC_{50} value for blockage of HERG K+ channels, log HERG, apparent Caco-2 cell permeability, QPP Caco in nm/s, metabolic reactions, #metab, Polarizability, QP polrz, Absorption, Distribution, Metabolism, Excretion, and Toxicity (ADME/T) properties of the selected best docked ligands molecules were predicted using QikProp tool of Schrodinger 2012. It predicted the properties such as the number of hydrogen bond acceptors (HBA), donors (HBD), QP log Po/w, skin permeability, log Kp, percentage of human oral absorption, etc.

Supplementary data

Supplementary data associated HRMS and NMR spectra of compounds (**3a**, **3b**, **4a**, **4b**, **5a**, **5b**, **7a**, **7b** and **9a–c**). The Crystallographic data for compound **9b** has been deposited with the Cambridge Crystallographic Data Centre, CCDC No. 1042893. Copies of the data can be obtained free of charge on application to CCDC, 12 Union Road, Cambridge CB2 1EZ, UK (fax: +44 (0) 1223 336033 or e-mail: deposit@ccdc.cam.ac.uk).

Acknowledgments Authors are thankful to the Director, Institute of Advanced Study in Science and Technology, Assam, India, for giving us the facility to carry out this work. Thanks are attributable to DBT, Govt. of India for financial support as a Project.

References

Balaji B, Hariharan S, Shah DB, Ramanathan M (2014) Discovery of potential and selective COX-1 inhibitory leads using pharmacophore modelling, in silico screening and in vitro evaluation. Eur J Med Chem 86:469–480

Balasubramaninan S, Aridoss G, Parthiban P, Ramalingam C, Kabilan S (2006) Synthesis and biological evaluation of novel benzimidazol/benzoxazolylethoxypiperidone oximes. Biol Pharm Bull 29(1):125–130

Bartoli S, Cipollone A, Squarcia A, Madami A, Fattori D (2009) Electrophilic bromination of meta-substituted anilines with n-bromosuccinimide: regioselectivity and solvent effect. Synthesis 8:1305–1308

Brogden RN, Clissold SP (1989) Flutamide. A preliminary review of its pharmacodynamic and pharmacokinetic properties, and therapeutic efficacy in advanced prostatic cancer. Drugs 38(2):185–203

Chen J, Kim J, Dalton JT (2005) Discovery and therapeutic promise of selective androgen receptor modulators. Mol Interv 5(3):173–188

Clegg NJ, Wongvipat J, Joseph J, Tran C, Ouk S, Dilhas A, Chen Y, Grillot K, Bischoff ED, Cai L, Aparicio A, Dorow S, Arora V, Shao G, Qian J, Zhao H, Yang G, Cao C, Sensintaffar J, Wasielewska T, Herbert MR, Bonnefous C, Darimont B, Scher HI, Smith-Jones P, Klang M, Smith ND, Stanchina ED, Wu N, Ouerfelli O, Rix PJ, Heyman RA, Jung ME, Sawyers CL, Hager JH (2012) ARN-509: a novel antiandrogen for prostate cancer treatment. Cancer Res 72(6):1494–1503

Cleve A, Luecking U, Baeurle S, Fritsch M, Schroeder J, Igl BW (2011) Preparation of substituted (heteroarylmethyl) thiohydantoins and uses thereof as anticancer drugs for prevention and treatment of uterine fibroids and myoma. PCT IntAppl WO 2011029782(A1):20110317

Dalton JT, Miller DD, Rakov I, Bohl C, Mohler ML (2008) Selective androgen receptor modulators, analogs and derivatives thereof and uses thereof. Patent WO 2008011072:A2

Elancheran R, Das B, Kotoky J (2015a) CCDC 1042893: experimental crystal. Struct Determ. doi:10.5517/cc1406q2

Elancheran R, Maruthanila VL, Ramanathan M, Kabilan S, Devi R, Kunnumakkara A, Kotoky J (2015b) Recent discoveries and developments of androgen receptor based therapy for prostate cancer. Med Chem Comm 6(5):746–768

Ferlay J, Shin HR, Bray F, Forman D, Mathers C, Parkin DM (2010) Estimates of worldwide burden of cancer in 2008: GLOBOCAN 2008. Int J Cancer 127(12):2893–2917

Figg WD, Chau CH, Small EJ (2010) Drug Management of Prostate Cancer P–71

Fioretti FM, Sita-Lumsden A, Bevan CL, Brooke GN (2014) Revising the role of the androgen receptor in breast cancer. J Mol Endocrinol 52(3):R257–R265

Friesner RA, Banks JL, Murphy RB, Halgren TA, Klicic JJ, Mainz DT, Repasky MP, Knoll EH, Shaw DE, Shelley M, Perry JK, Francis P, Shenkin PS (2004) Glide: a new approach for rapid, accurate docking and scoring. 1. Method and assessment of docking accuracy. J Med Chem 47(7):1739–1749

Friesner RA, Murphy RB, Repasky MP, Frye LL, Greenwood JR, Halgren TA, Sanschagrin PC, Mainz DT (2006) Extra precision glide: docking and scoring incorporating a model of hydrophobic enclosure for protein–ligand complexes. J Med Chem 49(21):6177–6196

Gao W, Kim J, Dalton JT (2006) Pharmacokinetics and pharmacodynamics of nonsteroidal androgen receptor ligands. Pharm Res 23(8):1641–1658

Garay JP, Park BH (2012) Androgen receptor as a targeted therapy for breast cancer. Am J Cancer Res 2(4):434–445

Guo C, Pairish M, Linton A, Kephart S, Ornelas M, Nagata A, Burke B, Dong L, Engebretsen J, Fanjul AN (2012) Design of oxobenzimidazoles and oxindoles as novel androgen receptor antagonists. Bioorg Med Chem Lett 22(7):2572–2578

Halgren TA, Murphy RB, Friesner RA, Beard HS, Frye LL, Pollard WT, Banks JL (2004) Glide: a new approach for rapid, accurate docking and scoring. 2. Enrichment factors in database screening. J Med Chem 47(7):1750–1759

Howlader N, Noone AM, Krapcho M, Garshell J, Neyman N, Altekruse SF, Kosary CL, Yu M, Ruhl J, Tatalovich Z, Cho H, Mariotto A, Lewis DR, Chen HS, Feuer EJ, Cronin KA (2015) SEER Cancer Statistics Review: 1975–2012 National Cancer Institute. Bethesda MD, http://seer.cancer.gov/csr/1975_2012/ based on November 2014 SEER data submission, posted to the SEER web site, April 2015

Hsieh AC, Ryan CJ (2008) Novel concepts in androgen receptor blockade. Cancer J 14(1):11–14

Ishioka T, Kubo A, Koiso Y, Nagasawa K, Itai A, Hashimoto Y (2002) Novel non-steroidal/non-anilide type androgen antagonists with an isoxazolone moiety. Bioorg Med Chem 10(5):1555–1566

Jésus-Tran KP, Côté P, Cantin L, Blanchet J, Labrie F, Breton R (2006) Comparison of crystal structures of human androgen receptor ligand-binding domain complexed with various agonists reveals molecular determinants responsible for binding affinity. Protein Sci 15(5):987–999

Jorgensen WL, Duffy EM (2002) Prediction of drug solubility from structure. Adv Drug Deliv Rev 54(3):355–366

Kassouf W, Tanguay S, Aprikian AG (2003) Nilutamide as second line hormone therapy for prostate cancer after androgen ablation fails. J Urol 169(5):1742–1744

Khanfar MA, Sayed KAE (2010) Phenylmethylene hydantoins as prostate cancer invasion and migration inhibitors. CoMFA approach and QSAR analysis. Eur J Med Chem 45(11):5397–5405

Khatik GL, Kaur J, Kumar V, Tikoo K, Venugopalan P, Nair VA (2011) Aldol derivatives of Thioxoimidazolidinones as potential anti-prostate cancer agents. Eur J Med Chem 46(8):3291–3301

Moguilewsky M, Bertagna C, Hucher M (1987) Pharmacological and clinical studies of the antiandrogen Anandron (nilutamide). J Steroid Biochem 27(4–6):871–875

Mosmann T (1983) Rapid colorimetric assay for cellular growth and survival: application to proliferation and cytotoxicity assays. J Immunol Methods 65(1–2):55–63

Neumann F, Töpert M (1986) Pharmacology of antiandrogens. J Ster Biochem 25(5B):885–895

Ni M, Chen Y, Lim E, Wimberly H, Bailey ST, Imai Y, Rimm DL, Liu XS, Brown M (2011) Targeting androgen receptor in estrogen receptor-negative breast cancer. Cancer Cell 20(1):119–131

Niemeier LA, Dabbs DJ, Beriwal S, Striebel JM, Bhargava R (2010) Androgen receptor in breast cancer: expression in estrogen receptor-positive tumors and in estrogen receptor-negative tumors with apocrine differentiation. Mod Pathol 23(2):205–212

Nunez-Nateras R, Castle EP (2011) Genitourinary Cancers Symposium, American Society of Clinical Oncology, Florida, USA, 2011, Abstract 168

Piatnitski Chekler EL, Unwalla R, Khan TA, Tangirala RS, Johnson M, St Andre M, Anderson JT, Kenney T, Chiparri S, McNally C, Kilbourne E, Thompson C, Nagpal S, Weber G, Schelling S, Owens J, Morris CA, Powell D, Verhoest PR, Gilbert AM (2014) 1-(2-Hydroxy-2-methyl-3-phenoxypropanoyl)indoline-4-carbonitrile derivatives as potent and tissue selective androgen receptor modulators. J Med Chem 57(6):2462–2471

Rubeinstein LV, Shoemaker RH, Paul KD, Simo RM, Tosini S, Skehan P, Scudiero PA, Monks A, Boyd MR (1990) Comparison of in vitro anticancer-drug-screening data generated with a tetrazolium assay versus a protein assay against a diverse panel of human tumor cell lines. J Natl Cancer Inst 82(13):1113–1117

Schayowitz A, Sabnis G, Njar VCO, Brodie AMH (2008) Synergistic effect of a novel antiandrogen, VN/124-1, and signal transduction inhibitors in prostate cancer progression to hormone independence in vitro. Mol Cancer Ther 7(1):121–132

Scher HI, Beer TM, Higano CS, Anand A, Taplin ME, Efstathiou E, Rathkopf D, Shelkey J, Yu EY, Alumkal J, Hung D, Hirmand M, Seely L, Morris MJ, Danila DC, Humm J, Larson S, Fleisher M, Sawyers CL (2010) Antitumour activity of MDV3100 in castration-resistant prostate cancer: a phase 1–2 study. Lancet 375(9724):1437–1446

Schrödinger (2013) LLC: New York, NY. Glide, version 6.1
Sheldrick GM (1990) Phase annealing in shelx-90: direct methods for larger structures. Acta Crystallogr A 46:467
Sheldrick GM (1997) shelx-97: Program for the refinement of crystal structures. Universitaèt of Goèttingen, Germany **1997**
Tran C, Ouk S, Clegg NJ, Chen Y, Watson PA, Arora V, Wongvipat J, Smith-Jones PM, Yoo D, Kwon A, Wasielewska T, Welsbie D, Chen CD, Higano CS, Beer TM, Hung DT, Scher HI, Jung ME, Sawyers CL (2009) Development of a second-generation antiandrogen for treatment of advanced prostate cancer. Science 324(5928):787–790